FUDMA Journal of Sciences (FJS)
ISSN online: 2616-1370
ISSN print: 2645 - 2944
Vol. 10 No. 4, February, 2026, pp 21 – 29
DOI: https://doi.org/10.33003/fjs-2026-1004-4835

SHORELINE EXTRACTION FROM HIGH-RESOLUTION OPTICAL IMAGERY USING A U-NET-BASED SEMANTIC SEGMENTATION APPROACH

[1]Godsent Efosa Felix, [1]Destiny Osazee, [2]Uchenna Ukeme and *[1]Stephen Olushola Oladosu

[1]University of Benin, Faculty of Environmental Sciences, Department of Geomatics, Benin, Edo State, Nigeria.
[2] University of Benin, Faculty of Engineering, Department of Civil Engineering, Benin, Edo State, Nigeria.

*Corresponding Authors' Email: olushola.oladosu@uniben.edu Phone: +2348065211810

ABSTRACT

Accurate shoreline delineation is fundamental for coastal monitoring, environmental management, and hazard mitigation. This study presents a deep learning–based semantic segmentation framework for automated shoreline extraction from high-resolution optical imagery using a U-Net architecture. A dataset comprising 31 manually annotated coastal images was augmented through geometric transformations to generate 155 image–mask pairs for model training, validation, and testing. The network was optimized using the Adam optimizer and a hybrid Dice–Binary Cross-Entropy loss function to mitigate class imbalance between land and water pixels. Model performance was evaluated using Accuracy, Precision, Recall, F1-score, and Intersection over Union (IoU) metrics. Validation results demonstrated strong segmentation performance, achieving an Accuracy of 98.63%, Precision of 83.58%, Recall of 81.75%, and F1-score of 81.93%. On an independent test dataset representing diverse coastal environments, the model attained an Accuracy of 98.33% and an F1-score of 78.24%, indicating robust generalization under heterogeneous imaging conditions. Despite the limited dataset size, the results confirm the methodological feasibility and reliability of U-Net-based semantic segmentation for shoreline delineation. The proposed framework offers a reproducible and computationally efficient foundation for scalable shoreline mapping and future multi-temporal coastal monitoring applications.

Keywords: Keyword Automatedb, Google Earth, Semantic segmentation, Binary segmentation, Coastline delineation

INTRODUCTION

Coastal zones represent some of the most dynamic and environmentally sensitive regions on Earth, shaped by the continuous interaction of natural processes and anthropogenic activities. These environments provide critical ecological services, serve as economic hubs, and support a rapidly growing proportion of the global population (Maul & Duedall, 2019; Cosby *et al.*, 2024). However, accelerated urbanization, coastal engineering, sea-level rise, intensified storm events, and sediment transport imbalance have significantly altered shoreline positions worldwide, resulting in widespread coastal erosion, habitat degradation, and increased vulnerability to flooding and storm surges (Asensio-Montesinos *et al.*, 2024; Balakrishnan *et al.*, 2023; Angnuureng *et al.*, 2025). Accurate, timely, and scalable shoreline monitoring is therefore essential for effective coastal zone management, disaster risk reduction, and sustainable development planning (Kundu & Mandal, 2024; Zhang *et al.*, 2024).

Traditional shoreline mapping approaches have relied on ground surveys, aerial photogrammetry, and manual interpretation of topographic maps and satellite imagery. While these techniques can achieve high positional accuracy, they are often labor-intensive, time-consuming, and costly, limiting their suitability for frequent large-scale monitoring (McAllister *et al.*, 2022; Liu *et al.*, 2024). Advances in remote sensing technologies, including multispectral satellite imaging, airborne LiDAR, unmanned aerial vehicle (UAV) photogrammetry, and synthetic aperture radar (SAR), have substantially enhanced spatial resolution and temporal coverage for shoreline observation. Since the launch of the Earth Resources Technology Satellite (ERTS-1, now Landsat 1) in 1972, Earth observation systems have continuously evolved, leading to the current availability of diverse satellite platforms such as Landsat 8 and 9, Sentinel-1 and Sentinel-2, and high-resolution commercial constellations including PlanetScope and WorldView (Belward & Skøien, 2015; Alan *et al.*, 2015; Ustin & Middleton, 2024; Christofi *et al.*, 2025). These advances have enabled unprecedented opportunities for systematic and scalable coastal monitoring.

Despite these technological developments, automated shoreline extraction from satellite imagery remains challenging. Early computational approaches relied predominantly on pixel-based thresholding techniques, such as the Normalized Difference Water Index (NDWI), band ratio methods, and classical edge detection algorithms, as well as conventional supervised machine learning classifiers (McAllister *et al.*, 2022; Zhou *et al.*, 2023). While these methods perform satisfactorily under optically simple conditions, their effectiveness degrades markedly in heterogeneous coastal environments characterized by variable water turbidity, wet sand reflectance, shadow effects, and complex shoreline morphology (Dang *et al.*, 2022; Liu *et al.*, 2024). These limitations often lead to fragmented shorelines, reduced boundary continuity, and limited generalization across geographically diverse coastal regions, highlighting the need for more adaptive and robust shoreline extraction frameworks.

Recent advances in deep learning, particularly convolutional neural networks (CNNs), have revolutionized remote sensing image analysis by enabling automatic hierarchical feature learning and robust generalization across complex scenes. Semantic segmentation architectures, including U-Net, U-Net++, Attention U-Net, and DeepLabV3+, have demonstrated exceptional performance in pixel-level classification tasks such as land cover mapping, road extraction, surface water detection, and coastline delineation (Liu *et al.*, 2024; Yang *et al.*, 2024; Santos *et al.*, 2025; Mahmoud *et al.*, 2025). Among these architectures, U-Net has gained widespread adoption due to its relatively simple design, strong localization capability, and effectiveness under limited training data conditions. Originally developed for

biomedical image segmentation, U-Net and its variants have been successfully adapted to diverse geospatial applications, including shoreline extraction, offering precise boundary delineation even in visually complex environments (Ronneberger *et al.*, 2015; Çiçek *et al.*, 2016; Liu *et al.*, 2024). Although deep learning–based shoreline extraction methods have shown considerable promise, several critical challenges persist. Many existing studies rely on large, sensor-specific datasets, complex multi-input network architectures, or regionally constrained case studies, which may limit computational efficiency, reproducibility, and applicability in data-scarce environments (Christofi *et al.*, 2025; Mahmoud *et al.*, 2025).

Furthermore, relatively few studies have systematically evaluated the performance of lightweight, reproducible U-Net-based segmentation frameworks using high-resolution optical imagery obtained from globally accessible platforms. Such imagery often represents the primary data source available for coastal studies in developing regions, where access to calibrated multispectral or SAR datasets may be restricted. In addition, limited attention has been directed toward assessing generalization performance under heterogeneous environmental conditions when training data availability is constrained, creating a notable methodological gap.

To address these limitations, this study proposes a deep learning–based semantic segmentation framework for automated shoreline extraction from high-resolution optical imagery using a U-Net architecture. The framework integrates geometric data augmentation, hybrid loss optimization, and post-processing-based shoreline vectorization to enable accurate, continuous, and computationally efficient shoreline delineation. Unlike site-specific or multi-temporal shoreline change studies, the present work adopts a methodological focus, emphasizing algorithm development, performance evaluation, and generalization capability across diverse coastal imaging conditions. The main contributions of this study are threefold: (i) development of a reproducible U-Net-based segmentation framework tailored for shoreline extraction under limited data availability; (ii) comprehensive quantitative evaluation using multiple performance metrics across training, validation, and independent testing datasets; and (iii) demonstration of an end-to-end shoreline extraction pipeline integrating deep learning segmentation with vector-based post-processing suitable for GIS-based coastal analysis. The proposed framework provides a robust methodological foundation for scalable shoreline mapping and future multi-temporal coastal monitoring applications.

MATERIALS AND METHODS

Conceptual Study Framework and Data Scope

This study adopts a methodological, data-driven framework rather than a site-specific coastal case study. The objective is to develop and evaluate a deep learning–based shoreline extraction approach that is applicable across a range of coastal image conditions. Accordingly, the analysis is conducted at the image and pixel levels, without restricting the investigation to a single, geographically continuous shoreline segment.

The dataset comprises high-resolution optical imagery representing diverse coastal settings, including sandy beaches, estuarine margins, and anthropogenically modified shorelines typical of low-lying tropical and subtropical environments. Images were selected to capture variability in shoreline morphology, land–water contrast, and environmental complexity, thereby enabling a more comprehensive assessment of model performance under heterogeneous conditions.

High-resolution optical imagery was obtained from Google Earth Pro for methodological development and evaluation purposes. Although Google Earth imagery does not provide standardized sensor metadata or guaranteed positional accuracy, it offers visually interpretable, high-resolution data suitable for testing automated shoreline extraction algorithms. In this study, the use of Google Earth imagery is strictly limited to algorithm development and performance evaluation, rather than absolute shoreline position measurement or site-specific coastal change analysis.

Image Source and Dataset Description

High-resolution optical imagery used in this study was obtained from Google Earth Pro and selected for methodological development and evaluation of shoreline segmentation. Image selection was guided by visual criteria, including minimal cloud cover, clear land–water contrast, and the presence of distinct shoreline features.

To enhance the diversity of shoreline characteristics represented in the dataset, imagery was sampled from multiple, spatially independent coastal settings exhibiting variations in shoreline morphology, surface texture, and environmental conditions. Although Google Earth imagery does not provide standardized sensor metadata, its high spatial detail and visual interpretability are suitable for assessing the performance of automated shoreline extraction algorithms at the image level.

Data Size Preprocessing and Annotation

Although the original dataset comprises only 31 manually annotated coastal images, the objective of this study is methodological development and feasibility assessment rather than large-scale operational deployment. Prior studies have demonstrated that U-Net-based architectures can achieve reliable segmentation performance even under limited training data conditions when supported by appropriate data augmentation strategies (Ronneberger *et al.*, 2015; Liu *et al*., 2024). In this study, extensive geometric augmentation was applied to improve feature diversity and generalization capability. Nevertheless, future extensions of this framework should incorporate larger and more geographically diverse datasets, as well as cross-validation strategies, to further strengthen statistical robustness and generalization performance. The acquired imagery was preprocessed using ArcGIS 10.4 to isolate coastal zones of interest and to ensure consistent input dimensions for model training. Each image was manually cropped to focus on land–water interfaces while minimizing irrelevant inland or offshore areas.

Ground-truth shoreline masks were generated through manual annotation, in which pixels were classified into binary land and water classes. These annotated masks served as supervisory labels for training and evaluating the deep learning model. The annotation process was performed consistently across all images to maintain label coherence. Figure 1shows a representative examples of high-resolution optical coastal imagery used in this study and their corresponding manually annotated for shoreline segmentation.

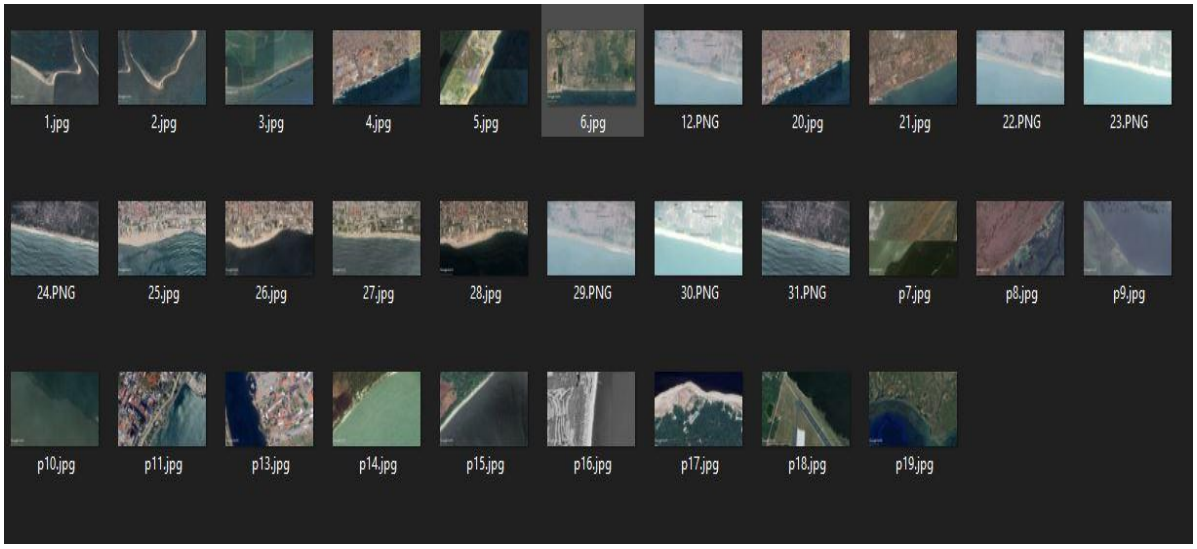

Figure 1: Image Preparation Phase

To improve model robustness and generalization, the initial dataset of 31 manually annotated images was augmented using geometric transformations, including horizontal and vertical flipping, rotation, and scaling. Data partitioning into training, validation, and testing subsets was performed prior to augmentation using a 70:10:20 ratio to prevent information leakage between datasets. Augmentation was then applied independently to each subset, resulting in a total of 155 image–mask pairs. To improve statistical robustness despite the limited dataset size, stratified k-fold cross-validation could be adopted in future extensions of this work to further validate generalization performance across heterogeneous coastal environments.

All images and corresponding masks were resized to 512 × 512 pixels to ensure uniform input dimensions for model training. Pixel intensity values were normalized on a per-image basis to improve numerical stability during training, as expressed in equation (1):

$$I_{norm} = \frac{I - I_{min}}{Imin_{max}} \quad (1)$$

Where: I represents the original pixel intensity, and $I_{\min}$ and $I_{\max}$ are the minimum and maximum pixel values in the image.

U-Net Architecture and Segmentation Process

Shoreline segmentation in this study was carried out using a U-Net convolutional neural network, selected for its effectiveness in pixel-level semantic segmentation tasks, particularly when training data are limited (Ronneberger *et al*., 2015). The U-Net architecture employs a symmetric encoder–decoder structure with skip connections that facilitate the preservation of fine spatial details, which is essential for delineating complex land–water boundaries.

As illustrated in Figure 2, the network consists of a contracting path (encoder) for hierarchical feature extraction and an expansive path (decoder) for spatial resolution recovery. Feature extraction in the encoder is performed through successive convolutional layers followed by nonlinear activation and downsampling operations. The transformation at layer $l$can be expressed as expressed in equation 2:

$$F_l = \sigma(BN(W_l * F_{l-1} + b_l) \quad (2)$$

Where: F_l is the feature map at layer l, W_l and b_l are the convolutional weights and bias respectively, $BN(\cdot)$denotes batch normalization, $*$indicates convolution, and $\sigma(\cdot)$is the Rectified Linear Unit (ReLU) activation function.

At the network bottleneck, deeper layers capture high-level semantic representations of coastal features. The decoder path restores spatial resolution through transposed convolution, while skip connections concatenate corresponding encoder feature maps with decoder outputs to preserve shoreline delineation and/or boundary-related information (Çiçek e*t al*., 2016). The final segmentation output is generated using a sigmoid activation function to produce a pixel-wise shoreline probability map, as shown in equation (3):

$$\boldsymbol{P(x)} = \frac{\mathbf{1}}{\mathbf{1}+\boldsymbol{e}^{-\boldsymbol{x}}} \quad (3)$$

Where: x is the input to the sigmoid function.

Figure 3 presents the complete shoreline extraction workflow, including data preprocessing, model training, and segmentation output generation.

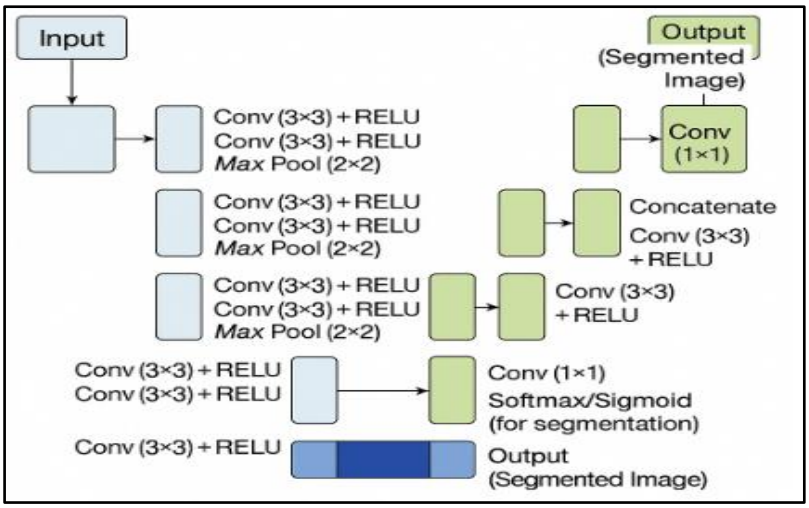

Figure 2: Adopted U-Net Architecture for the Study

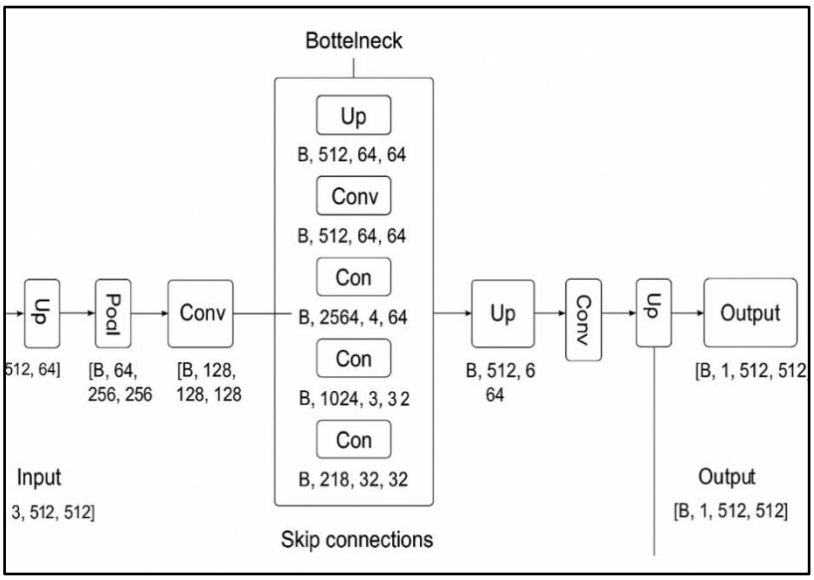

Figure 3: U-Net Model Pipeline for Shoreline Detection

Model Training and Loss Optimization

Model training was conducted using the Adam optimization algorithm with a learning rate of $1 \times 10^{-4}$and a batch size of 8. The network was trained for 200 epochs on a GPU-enabled Google Colab Pro environment.

To mitigate class imbalance between land and water pixels and to enhance shoreline boundary delineation, a hybrid loss function combining Binary Cross-Entropy (BCE) loss and Dice loss was employed. The BCE loss, which penalizes pixel-wise classification errors, is defined as by equation (4):

$$\mathcal{L}_{\text{BCE}} = -\frac{1}{N}\sum_{i=1}^{N}[y_i \log(p_i) + (1-y_i)\log(1-p_i)] \quad (4)$$

Where L_{BCE} denote the Binary Cross-Entropy, $y_i$is the ground-truth label, $p_i$is the predicted probability, and $N$is the total number of pixels.

Dice loss, which emphasizes spatial overlap between predicted and reference masks, is given by equation (5):

$$\mathcal{L}_{\text{Dice}} = 1 - \frac{2\,TP}{2\,TP+FP+FN} \quad (5)$$

Where TP, FP, and FNdenote true positives, false positives, and false negatives, respectively.

The combined loss function used for model optimization is expressed as in equation 6:

$$\mathcal{L} = \alpha\mathcal{L}_{\text{BCE}} + (1-\alpha)\mathcal{L}_{\text{Dice}} \quad (6)$$

Where αcontrols the relative contribution of each loss component. Early stopping and model checkpointing were applied based on validation Dice performance to reduce overfitting.

Post-Processing and Shoreline Vectorization

The pixel-wise probability maps produced by the U-Net model were post-processed to generate continuous shoreline representations suitable for subsequent analysis. Post-processing included thresholding the sigmoid output at 0.5 to obtain binary land–water masks, morphological operations to remove isolated pixels and small artifacts, and edge smoothing to reduce jagged boundaries caused by pixel-level predictions. The resulting binary masks were then vectorized into polylines using Python libraries (OpenCV and Shapely), enabling extraction of coastline coordinates and integration with further computational analyses. This fully Python-based workflow ensures reproducibility and allows the extracted shorelines to be readily used in visualization, spatial analysis, or other downstream applications. Binarization of probability maps was performed using equation (7):

$$M(x) = \begin{cases} 1, P(x) \geq 0.5 \\ 0, P(x) < 0.5 \end{cases} \quad (7)$$

Morphological opening and closing operations were applied to suppress isolated noise and smooth boundary irregularities in the binary segmentation outputs. Skeletonization was subsequently employed to reduce the segmented shoreline regions to a one-pixel-wide centerline, after which contour detection algorithms were used to extract continuous shoreline boundaries.

Vectorization was carried out using Python-based libraries, including OpenCV and Shapely, resulting in polyline representations of the extracted shorelines. The vector outputs were saved in standard formats to support visualization and subsequent computational analysis, without implying positional accuracy or map-based validation.

Performance Evaluation Metrics

Model performance was assessed using Intersection over Union (IoU), as shown in equation (8):

$$IoU = \frac{|\hat{M} \cap M|}{|\hat{M} \cup M|} = \frac{TP}{TP+FP+FN} \quad (8)$$

Where: TP, FP, and FN denote true positives, false positives, and false negatives.

Additional metrics including accuracy, precision, and recall were calculated using equations (9)-(11):

$$Accuracy = \frac{TP+TN}{TP+TN+FP+FN} \quad (9)$$

$$Pr\,e\,cision = \frac{TP}{TP+FP} \quad (10)$$

$$Re\,c\,all = \frac{TP}{TP+FN} \quad (11)$$

Shoreline Change Quantification

This study focuses on the development and evaluation of a deep learning–based shoreline extraction methodology and does not include multi-temporal shoreline change analysis. However, to demonstrate the extensibility of the proposed framework, a conceptual formulation for shoreline change quantification is briefly outlined.

For potential future applications involving multi-date shoreline datasets, shoreline change between two epochs t_1 and t_2 can be expressed as shown in equation 12:

$$\Delta S = S_{t_2} - S_{t_1} \quad (12)$$

Where S_{t_1} and S_{t_2} represent shoreline positions at different times.

Following vectorization, shoreline geometry may be represented as an ordered polyline of N points, with total shoreline length L computed using Euclidean distance represented by equation (13):

$$L = \sum_{i=1}^{N-1} \sqrt{(x_{i+1} - x_i)^2 + (y_{i+1} - y_i)^2} \quad (13)$$

RESULTS AND DISCUSSION

Model Training, Validation, and Convergence Behaviour

The U-Net model was trained using a dataset of 31 manually annotated high-resolution coastal images and corresponding land–water masks, with data augmentation applied to mitigate limitations associated with the relatively small sample size. Model training followed the configuration described in Section 2, and performance was evaluated using independent training and validation subsets.

The learning curves for both accuracy and loss demonstrate a smooth and stable convergence pattern, with training and validation curves closely aligned throughout the training process. This behaviour indicates that the network successfully learned meaningful spatial and spectral representations of land–water boundaries without exhibiting significant overfitting. Such convergence stability is consistent with findings in deep learning–based shoreline extraction studies, where properly regularized U-Net architectures have been shown to generalize effectively even with limited training data (Liu *et al*., 2024; Santos *et al.*, 2025).

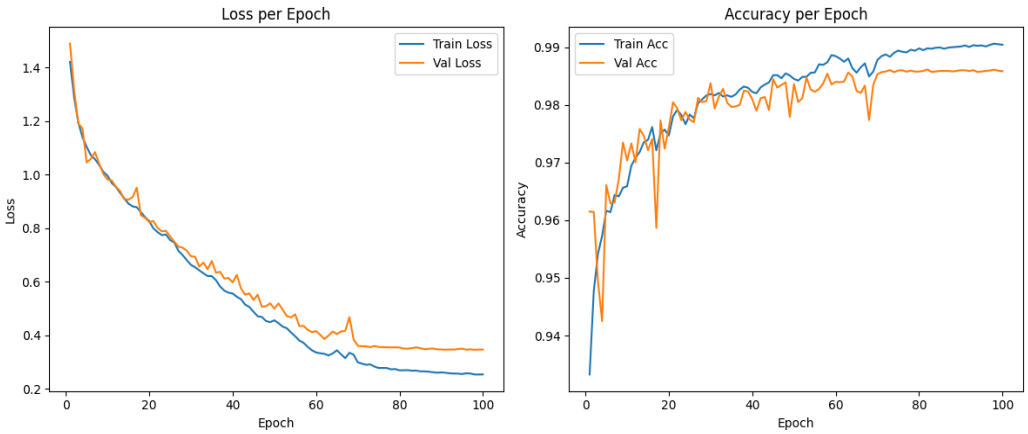

Figure 4: Accuracy vs. Epoch (Training & Validation) & Loss vs. Epoch (Training & Validation)

Quantitative evaluation on the validation dataset yielded an Accuracy of 98.63%, Precision of 83.58%, Recall of 81.75%, and an F1-score of 81.93%. While the high accuracy reflects overall classification performance, it is important to note that accuracy is influenced by class imbalance, as water pixels typically dominate coastal imagery. Consequently, metrics such as Precision, Recall, and F1-score provide a more reliable assessment of shoreline delineation performance.

The relatively close agreement between Precision and Recall indicates that the model achieved a balanced trade-off between commission and omission errors. The achieved validation metrics are comparable with, and in some cases exceed, those reported in recent studies applying convolutional neural networks for shoreline extraction across diverse coastal environments (Santos *et al*., 2025; Mahmoud *et al*., 2025; Liu *et al*., 2024). This confirms that the proposed framework is capable of accurately delineating land–water boundaries under controlled validation conditions.

Performance Under Testing and Environmental Variability

To further assess model robustness, performance was evaluated on an independent test dataset representing a range of environmental conditions, including turbidity, shadowing, and complex shoreline geometries.

On the test dataset, the model achieved an Accuracy of 98.33%, Recall of 88.01%, Precision of 71.49%, and an F1-score of 78.24%. The relatively high Recall indicates that the model effectively identified shoreline pixels across diverse environmental conditions, thereby minimizing omission errors and preserving shoreline continuity. This recall-dominant behaviour is particularly advantageous in coastal monitoring applications, where missing shoreline segments can introduce significant uncertainties in shoreline change analysis and hazard assessment (Mahmoud *et al*., 2025; Dang *et al*., 2022).

However, the comparatively lower Precision reflects the occurrence of false positive classifications, particularly in optically complex regions such as turbid nearshore waters, wet sand zones, and shadowed coastal areas. These environments reduce spectral contrast between land and water surfaces, thereby increasing classification uncertainty. Similar reductions in precision under heterogeneous coastal conditions have been widely reported in previous deep learning–based shoreline segmentation studies (Santos *et al.,* 2025; Dang *et al*., 2022).

Despite this limitation, the impact of commission errors can be effectively mitigated through post-processing techniques such as morphological filtering, contour smoothing, and spatial regularization, as implemented in the present framework. Representative examples of shoreline segmentation outputs under varying environmental conditions are presented in Figure 5.

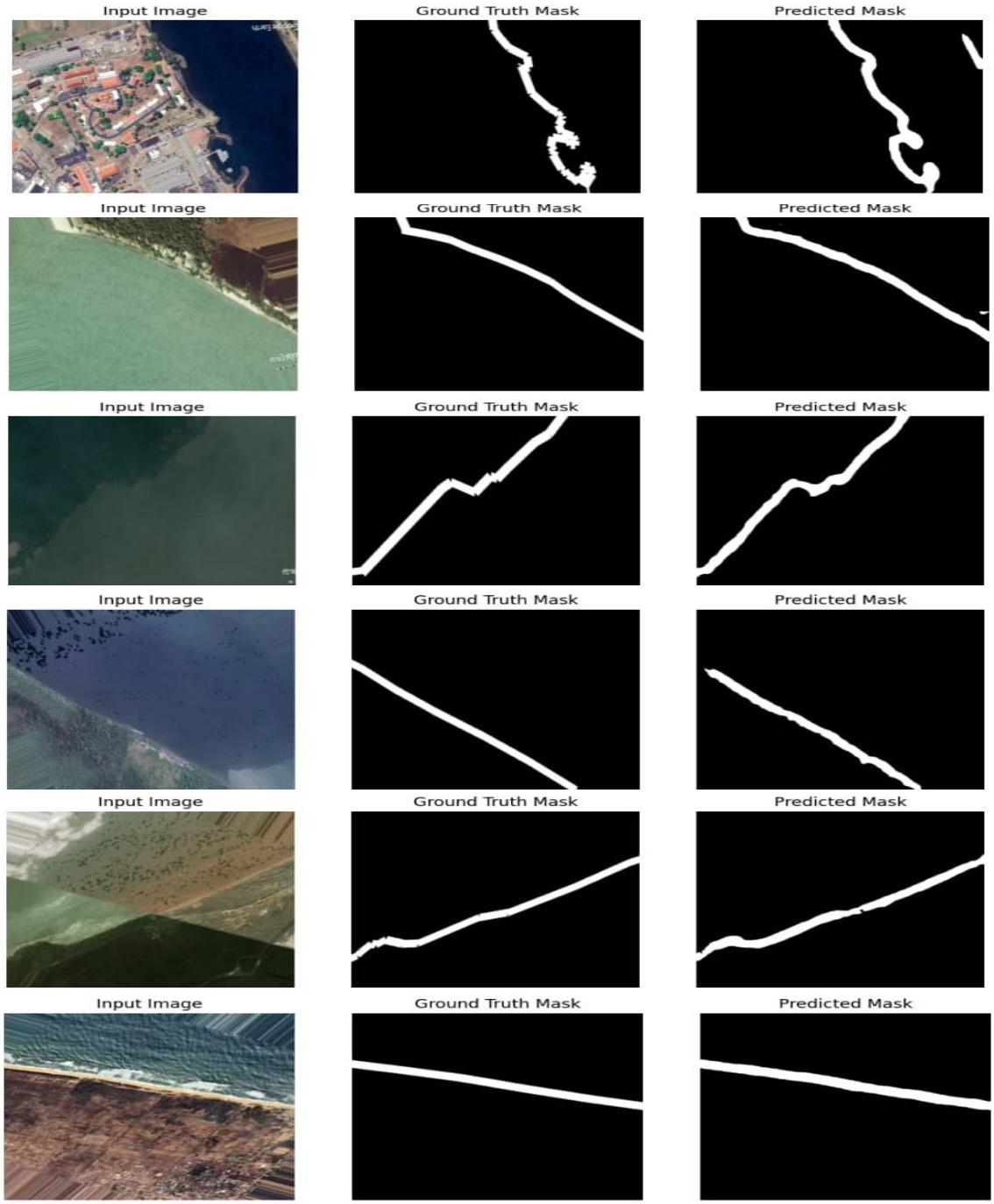

Figure 5: Representative of Model Performance for Shoreline Detection

Comparative Performance across Training, Validation, and Testing

A summary of performance metrics across training, validation, and testing phases is presented in Table 1. Accuracy values remained consistently above 98% across all phases, while F1-scores exceeded 78%, indicating stable and reliable model performance even under increasing data complexity. A gradual reduction in Precision and F1-score from training to testing is observed, which is expected due to the higher environmental variability present in real-world coastal imagery.

Notably, Recall values remained relatively high across all datasets, reinforcing the recall-dominant behaviour of the model. This characteristic is considered desirable in shoreline extraction tasks, as preserving shoreline continuity is often more critical than minimizing false detections (Mahmoud *et al.*, 2025; Dang *et al*., 2022).

Table 1: Performance Metrics: Training, Validation, and Testing

Metric	Training (%)	Validation (%)	Testing (%)
Accuracy	99.0	98.5	98.7
Precision	81.6	78.2	81.21
Recall	97.5	87.52	81.37
F1-score	88.8	82.62	79.3

Note: Metrics reported in Table 1 represent averaged values computed over all samples within each dataset, whereas values reported in Sections 3.1 and 3.2 correspond to the best-performing training epoch.

When compared with traditional shoreline extraction approaches such as NDWI thresholding, edge detection algorithms, and classical machine learning classifiers, the proposed U-Net-based framework demonstrates clear methodological advantages. Conventional techniques often exhibit limited adaptability to spatial complexity, illumination variability, and sediment heterogeneity, typically achieving F1-scores in the range of 60–75% in optically complex coastal environments (Dang *et al.*, 2022; Zhou *et al*., 2023).

In contrast, the deep learning framework presented in this study consistently achieved F1-scores exceeding 78% on independent test data while maintaining strong shoreline continuity. This improvement can be attributed to the model's ability to integrate spectral, spatial, and contextual information through hierarchical feature learning, enabling robust generalization beyond simple pixel-based thresholding. Similar performance gains have been reported in recent studies utilizing convolutional neural networks for shoreline and surface water extraction (Liu *et al.*, 2024; Santos *et al.*, 2025).

Computational Efficiency and Practical Implications

The computational efficiency of the proposed framework further enhances its applicability for large-scale coastal monitoring. The use of a lightweight U-Net architecture, combined with GPU-accelerated inference, enables rapid shoreline segmentation across large image collections. This scalability is essential for regional to continental-scale applications, particularly in the context of increasing coastal vulnerability driven by sea-level rise, storm impacts, and anthropogenic activities.

Comparable operational advantages have been reported in recent real-time and near real-time deep learning–based shoreline extraction studies (Abujayyab, 2025; Santos *et al.*, 2025), highlighting the growing role of AI-driven approaches in coastal monitoring systems.

Limitations and Future Research Directions

Despite the promising results, several limitations should be acknowledged. First, the relatively small dataset size limits representation of diverse global shoreline morphologies and environmental conditions. Second, reliance on Google Earth imagery restricts access to sensor metadata and geometric calibration, which constrains positional accuracy and prevents rigorous geodetic validation. Third, the exclusive use of optical imagery makes the model sensitive to atmospheric effects, turbidity, and illumination variability.

Future research should therefore focus on integrating larger and more diverse datasets, including multispectral and synthetic aperture radar (SAR) imagery, to improve robustness under challenging observational conditions. Additionally, incorporating cross-validation strategies and geodetically calibrated datasets would support more rigorous performance assessment and enable accurate multi-temporal shoreline change analysis.

The findings of this study confirm that the proposed U-Net-based semantic segmentation framework provides a reliable, efficient, and scalable solution for automated shoreline extraction. Its strong generalization capability, recall-dominant performance, and compatibility with standard GIS workflows make it highly suitable for supporting large-scale coastal monitoring and environmental management initiatives.

CONCLUSION

This study presents a deep learning–based semantic segmentation framework for automated shoreline extraction from high-resolution optical imagery, employing a U-Net architecture optimized with data augmentation and a hybrid Dice–Binary Cross-Entropy loss function. The experimental results demonstrate consistently high segmentation accuracy across training, validation, and independent testing datasets, with overall accuracies exceeding 98% and robust F1-scores under diverse coastal imaging conditions. These findings confirm the effectiveness of convolutional neural networks in delineating complex land–water boundaries within heterogeneous coastal environments.

Despite the limited dataset size, the model exhibited strong generalization capability and stable convergence behaviour, indicating successful learning of discriminative shoreline features. The recall-dominant performance observed under testing conditions ensured preservation of shoreline continuity, which is critically important for reliable coastal erosion and accretion assessment. Although reduced precision was observed in optically challenging environments characterized by turbid waters, wet sand reflectance, and shadow effects, these limitations are consistent with existing literature and can be effectively mitigated through post-processing refinement and multi-sensor data integration.

From an operational perspective, the proposed framework demonstrates high computational efficiency and scalability, enabling rapid shoreline mapping over extensive spatial domains. Compared with conventional threshold-based and edge-detection techniques, the deep learning–based approach

offers superior adaptability, robustness, and accuracy by jointly exploiting spectral and spatial contextual information. Furthermore, the compatibility of the framework with standard GIS workflows enhances its applicability for practical coastal monitoring, spatial analysis, and environmental management applications.

In summary, the proposed U-Net-based segmentation framework provides a reliable, efficient, and reproducible solution for automated shoreline extraction using high-resolution optical imagery. Future work should focus on extending the methodology to multi-temporal and multi-sensor datasets, incorporating SAR and multispectral imagery, and implementing rigorous geodetic validation to support precise shoreline change detection and long-term coastal evolution studies.

REFERENCES

Abujayyab, S. K. M. (2025). Deep learning–based semantic segmentation for surface water extraction from Sentinel-2 imagery: Case study of Kuş and Uluabat lakes, Türkiye. *Turkish Journal of Remote Sensing, 7*(1), 91–106. https://doi.org/10.51489/tuzal.1647078

Angelini, R., Angelats, E., Luzi, G., Masiero, A., Simarro, G., & Ribas, F. (2024). Development of methods for satellite shoreline detection and monitoring of megacusp undulations. *Remote Sensing, 16*(23), 4553. https://doi.org/10.3390/rs16234553

Angnuureng, D. B., Charuka, B., Almar, R., Dada, O. A., Asumadu, R., Agboli, N. A., & Ofosu, G. T. (2025). Challenges and lessons learned from global coastal erosion protection strategies. *iScience, 28*(4), 112055. https://doi.org/10.1016/j.isci.2025.112055

Asensio-Montesinos, F., Molina, R., Anfuso, G., Manno, G., & Lo Re, C. (2024). Natural and human impacts on coastal areas. *Journal of Marine Science and Engineering, 12*(11), 2017. https://doi.org/10.3390/jmse12112017

Balakrishnan, P., Abulibdeh, A., & Abul Kasem Kabir, T. (2023). Assessment of the impact of anthropogenic evolution and natural processes on shoreline dynamics using multi-temporal satellite images and statistical analysis. *Water, 15*(8), 1440. https://doi.org/10.3390/w15081440

Belward, A. S., & Skøien, J. O. (2015). Who launched what, when and why: Trends in global land-cover observation capacity from civilian Earth observation satellites. *ISPRS Journal of Photogrammetry and Remote Sensing, 103*, 115–128. https://doi.org/10.1016/j.isprsjprs.2014.03.009

Christofi, D., Mettas, C., Evagorou, E., Stylianou, N., Eliades, M., Theocharidis, C., Chatzipavlis, A., Hasiotis, T., & Hadjimitsis, D. (2025). A review of open remote sensing data with GIS, AI, and UAV support for shoreline detection and coastal erosion monitoring. *Applied Sciences, 15*(9), 4771. https://doi.org/10.3390/app15094771

Cosby, A. G., Lebakula, V., Smith, C. N., Wanik, D. W., Bergene, K., Rose, A. N., Swanson, D., & Bloom, D. E. (2024). Accelerating growth of human coastal populations at the global and continent levels: 2000–2018. *Scientific Reports, 14*, 22489. https://doi.org/10.1038/s41598-024-73287-x

Dang, K. B., Dang, V. B., Ngo, V. L., Vu, K. C., & Nguyen, H. D. (2022). Shoreline extraction using deep learning models from high-resolution remote sensing images. *Sensors, 22*(15), 5634. https://doi.org/10.3390/s22155634

Donchyts, G., Baart, F., Winsemius, H., Gorelick, N., Kwadijk, J., & van de Giesen, N. (2016). Earth's surface water change over the past 30 years. *Nature Climate Change, 6*(9), 810–813. https://doi.org/10.1038/nclimate3111

Google LLC, 2024. Google Earth Pro. https://www.google.com/earth/Accessed 15 August 2024

Kundu, K., Mandal, J.K. Shoreline Change Detection and Future Prediction of Sundarban Delta Using Remote Sensing Data and Digital Shoreline Analysis System. *J Indian Soc Remote Sens* 52, 485–503 (2024). https://doi.org/10.1007/s12524-024-01833-1

Li, J., Roy, D. P., Zhang, H. K., & Yan, L. (2019). Shoreline change detection using Landsat time series in a cloud computing environment. *Remote Sensing of Environment, 232*, 111302. https://doi.org/10.1016/j.rse.2019.111302

Liu, Y., Wang, C., Ye, M., & Han, R. (2024). Coastal zone classification based on U-Net and remote sensing. *Applied Sciences, 14*(16), 7050. https://doi.org/10.3390/app14167050

Mahmoud, A. S., Mohamed, S. A., Helmy, A. K., & Nasr, A. H. (2025). BDCN-UNet: Advanced shoreline extraction techniques integrating deep learning. *Earth Science Informatics*. https://doi.org/10.1007/s12145-024-01693-w

Maul, G. A., & Duedall, I. W. (2019). Demography of coastal populations. In C. W. Finkl & C. Makowski (Eds.), *Encyclopedia of coastal science* (pp. xx–xx). Springer. https://doi.org/10.1007/978-3-319-93806-6_115

McAllister, E., Payo, A., Novellino, A., Dolphin, T., & Medina-Lopez, E. (2022). Multispectral satellite imagery and machine learning for the extraction of shoreline indicators. *Coastal Engineering, 174*, 104102. https://doi.org/10.1016/j.coastaleng.2022.104102

Milletari, F., Navab, N., & Ahmadi, S.-A. (2016). V-Net: Fully convolutional neural networks for volumetric medical image segmentation. In *Proceedings of the 2016 Fourth International Conference on 3D Vision (3DV)* (pp. 565–571). IEEE. https://doi.org/10.1109/3DV.2016.79

Remote sensing shoreline extraction method based on an optimized DeepLabV3+ model: A case study of Koh Lan Island, Thailand. (2025). *Journal of Marine Science and Engineering, 13*(4), 665. https://doi.org/10.3390/jmse13040665

Santos, F., Cunha, T. R., & Baptista, P. (2025). Deep learning–based semantic segmentation for automatic shoreline extraction in coastal video monitoring systems. *Remote Sensing, 17*(23), 3865. https://doi.org/10.3390/rs17233865

Ustin, S. L., & Middleton, E. M. (2024). Current and Near-Term Earth-Observing Environmental Satellites, Their Missions, Characteristics, Instruments, and Applications. *Sensors, 24*(11), 3488. https://doi.org/10.3390/s24113488

Yang, F., Chen, G., & Duan, J. (2024). Skip-encoder and skip-decoder for detection transformer in optical remote sensing. *Remote Sensing*, *16*(16), 2884. https://doi.org/10.3390/rs16162884

Zhang, Y., Li, H., Li, D., Hou, X., Guo, P., & Guo, J. (2024). Evolutionary dynamics of island shoreline in the context of climate change: Insights from extensive empirical evidence. *International Journal of Digital Earth*, *17*(1). https://doi.org/10.1080/17538947.2024.2329816

Zhou, X., Wang, J., Zheng, F., Wang, H., & Yang, H. (2023). An Overview of Coastline Extraction from Remote Sensing Data. *Remote Sensing*, *15*(19), 4865. https://doi.org/10.3390/rs15194865